Article

pubs.acs.org/Biomac

Enteric Polymer Based on pH-Responsive Aliphatic Polycarbonate Functionalized with Vitamin E To Facilitate Oral Delivery of Tacrolimus

Menglin Wang,[†] Jin Sun,[‡] Yinglei Zhai,*[,§] He Lian,[§] Cong Luo,[†] Lin Li,[†] Yuqian Du,[†] Dong Zhang,[†] Wenya Ding,[†] Shuhong Qiu,[†] Yuhai Liu,[†] Longfa Kou,[†] Xiangfei Han,[†] Rongwu Xiang,[§] Yongjun Wang,[†] and Zhonggui He*[,†]

[†]Department of Pharmaceutical Sciences, School of Pharmacy, Shenyang Pharmaceutical University, No. 103, Wenhua Road, Shenyang, 110016, China

[‡]Municipal Key Laboratory of Biopharmaceutics, School of Pharmacy, Shenyang Pharmaceutical University, No. 103, Wenhua Road, Shenyang, 110016, China

[§]School of Medical Instrument, Shenyang Pharmaceutical University, No. 103, Wenhua Road, Shenyang, 110016, China

Supporting Information

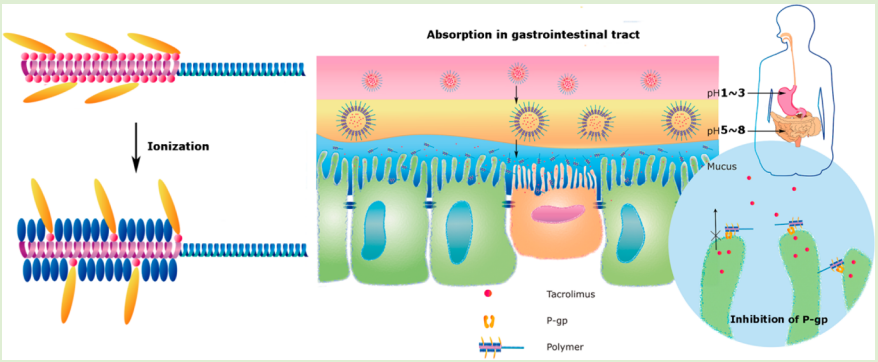

ABSTRACT: To improve the bioavailability of orally administered drugs, we synthesized a pH-sensitive polymer (poly(ethylene glycol)−poly(2-methyl-2-carboxyl-propylene carbonate)−vitamin E, mPEG−PCC−VE) attempting to integrate the advantages of enteric coating and P-glycoprotein (P-gp) inhibition. The aliphatic polycarbonate chain was functionalized with carboxyl groups and vitamin E via postpolymerization modification. Optimized by comparison and central composite design, $mPEG_{113}$−PCC_{32}−VE_4 exhibited low critical micelle concentration of 1.7×10^{-6} mg/mL and high drug loading ability for tacrolimus (21.2% ± 2.7%, w/w). The pH-responsive profile was demonstrated by pH-dependent swelling and *in vitro* drug release. Less than 4.0% tacrolimus was released under simulated gastric fluid after 2.5 h, whereas an immediate release was observed under simulated intestinal fluid. The $mPEG_{113}$−PCC_{32}−VE_4 micelles significantly increased the absorption of P-gp substrate tacrolimus in the whole intestine. The oral bioavailability of tacrolimus micelles was 6-fold higher than that of tacrolimus solution in rats. This enteric polymer therefore has the potential to become a useful nanoscale carrier for oral delivery of drugs.

INTRODUCTION

Nanometer-sized particles for drug delivery have been one of the major advancements in the past decade.[1] Poorly water-soluble drugs historically viewed as highly risky development candidates have a renaissance in oral delivery due to the new nanomedicine delivery strategy.[2] Abundant research has revealed superiority of polymeric micelles as nanovehicles for oral delivery, including small size, easy modification, lower toxicity, and reduced adverse reactions.[3] In contrast to the conventional small-molecule surfactants, the amphiphilic polymers furnish better kinetic and thermodynamic stability.[4] The hydrophobic cores of polymeric micelles solubilize poorly soluble drugs and defend them from the aqueous environment.[5] Among these, pH-sensitive polymeric micelles are better for oral drug delivery, since they maintain their structural stability in the stomach and are disassembled when they transit into small intestine.[6,7]

Most pH-sensitive biomedical micelles are related to polymers based on poly(methacrylic acid) (Eudragit, a commercial formulation of poly(methacrylic acid)),[8,9] poly(aspartic acid),[10] or poly(glutamic acid)[11] and recently reported polycaprolactone.[12] These polymers exhibit a pH-dependent ionization/dissociation profile due to functional carboxyl groups on their backbones or side chains. However, the pH-sensitive micelles

Received: December 19, 2014
Revised: February 25, 2015

DOI: 10.1021/bm501847u
Biomacromolecules XXXX, XXX, XXX−XXX

are mostly prepared in acidic media because of the repulsion among the ionized carboxyl groups.[13−15] It is a concern whether self-assembly could be induced in water by stronger hydrophobic attraction.

For the last two decades, aliphatic polycarbonates (APCs) together with other polyesters (polylactides,[16] polyglycolide,[17] poly(lactide-*co*-glycolide),[18] polydioxanone,[19] and polycaprolactone[20]) have been increasingly explored for biomedical applications as a consequence of their low toxicity, biodegradability, and biocompatibiliy.[18] The leading characteristics of APCs are low T_m, high susceptibility to hydrolysis, and elasticity. Additionally, degradation products of the conventional polyesters result in more detrimental acidity to loaded drugs or surrounding tissues.[21] By contrast, those of APCs are less stimulating, namely CO_2 and dihydric alcohol. Functional APCs have already been applied as an active component of sutures,[22] biodegradable elastomers,[23,24] and tissue engineering scaffolds.[25] Apart from applications as biocompatible engineering materials, APCs have been utilized as more versatile degradable carriers for drug delivery systems, such as floating microspheres,[26] injectable hydrogels,[27] and polymeric micelles.[28] Efficient postpolymerization modifications of APCs could open up new ways to fulfill their extended biomedical applications.[29] However, efforts have not been made to develop APCs as stimuli-responsive structures for oral drug delivery.

Vitamin E (VE) and its derivatives have shown their potential as drug carriers in recent years.[30] The biocompatibility and solubilizing capacity for poorly water-soluble drugs make VE a promising functional group for drug delivery systems.[31] As reported in the literature, VE has an inhibitory effect on cellular P-gp efflux pumps.[32,33] Our previous work showed that the newly developed amphiphilic VE derivatives (P_{5K}SSLV and PLV_{2K}) acted as P-gp ATPase reversible inhibitors.[34,35] Conjugating VE to APCs could enlarge the hydrophobic core volume as well as confer a P-gp inhibitory effect.

In this study, aliphatic polycarbonates functionalized with carboxyl and VE were prepared to exploit obvious pH-responsive behavior and P-gp inhibitory effect. Tacrolimus was selected because it is a potent substrate of P-gp and typical poorly water-soluble drug. As illustrated in Figure 1, the self-assembled micelles could stay compact and minimize the burst release of drug in the stomach. When the inner cores of pH-sensitive units ionized in the intestine, tacrolimus is rapidly released from the swelling micelles. The pH-responsiveness of poly(ethylene glycol)−poly(2-methyl-2-carboxyl-propylene carbonate)−vitamin E ($mPEG_{113}$−PCC_{32}−VE_4) micelles was realized by the competition between hydrophobic attraction and electrostatic repulsions. Further experiments were conducted to test the efficiency of this drug delivery system.

EXPERIMENTAL SECTION

Materials. Tacrolimus was obtained from Huifengda Chemical Corporation (Jinan, China). 2,2-Bis(hydroxoymethyl) propionic acid (DMPA; AR, 99%), and ethyl chloroformate (AR, 98%) were purchased from Ai Keda Chemical Technology (Chengdu, China). Benzyl chloride was procured from Rgent Chemicals (Tianjin, China). Potassium hydroxide (AR, 85%) was obtained from Hengxing Chemical Preparation (Tianjin, China). Poly(ethylene glycol) methyl ether (mPEG5000), average M_n 5000, was purchased from Sigma-Aldrich. 1,8-Diazabicyclo[5.4.0]undec-7-ene (99%) and Vitamin E (96%) were bought from Aladdin Industrial Corporation (Shanghai, China). Pa/C (10%) was obtained from Sinopharm Chemical Reagent (Beijing, China). Triethylamine (TEA, 99%) was obtained from Kermel Chemical Reagent (Tianjin, China). All other reagents were of analytical grade and used without other purification.

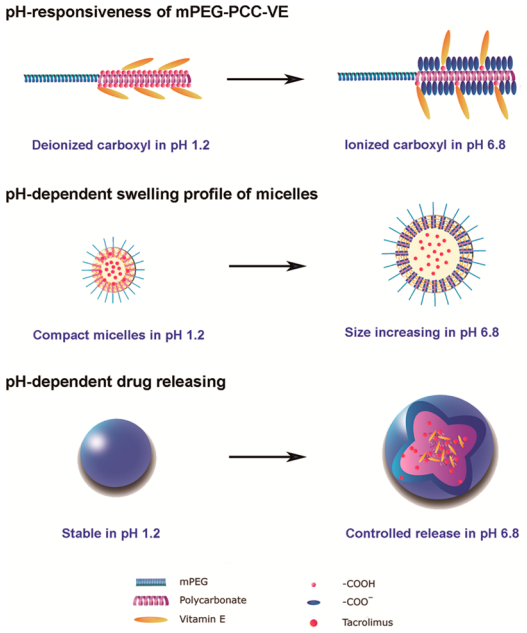

Figure 1. Schematic drawing of tacrolimus-loaded mPEG−PCC−VE micelles.

Methods. *Synthesis of mPEG−PCC−VE.* The 2-methyl-2-benzyloxycarbonyl-propylene carbonate (MBC) and poly(ethylene glycol)-*block*-poly(2-methyl-2-carboxyl-propylene carbonate) (mPEG−PCC) were synthesized mainly according to descriptions of Li et al., Danquah et al., and Guan et al.[36−38]

Synthesis of 5-Methyl-5-benzyloxycarbonyl-1,3-dioxane-2-one (BHP). DMPA (100.0 g, 0.738 mol) was dissolved in 370 mL of DMF in a flask. When DMPA was completely dissolved, 48.72 g (0.738 mol) of KOH was added into the flask with vigorous stirring at 100 °C. When all of the KOH reacted to form homogeneous potassium salt, 100.0 mL of benzyl chloride (0.790 mol) was dropwise added into the solution. The reaction was stirred for 12 h with efficient condensation in a 100 °C oil bath. Upon completion of the reaction, DMF was removed under vacuum. The residue was dissolved in a mixture of 480 mL of ethyl acetate, 480 mL of hexanes, and 300 mL of water. After extraction, the organic layer was washed with 100 mL of water and then dried with anhydrous sodium sulfate. With solvent evaporated, the remaining solid was recrystallized from toluene to produce BHP (121.0 g, yield 73.11%).

Synthesis of 2-Methyl-2-benzyloxycarbonyl-propylene Carbonate (MBC). BHP (60.0 g, 0.268 mol) and 130.1 mL of ethyl chloroformate (1.20 mol) was dissolved in 1000 mL of THF, and 123.9 mL of TEA diluted with 121.1 mL of THF was added dropwise in an ice bath. The reaction was controlled under 0 °C for 1 h then brought to room temperature for another 2 h. After filtration of the precipitate triethylamine hydrochloride, the residue was concentrated under vacuum and recrystallized from ether/THF (1:1) to give MBC (41.1 g, yield 61.38%).

Synthesis of Poly(ethylene glycol)-block-poly(2-methyl-2-benzoxycarbonyl-propylene carbonate) (mPEG−PBC). mPEG−PBC was synthesized by ring-opening polymerization. Initiator mPEG5000 (18.3 g, 0.00366 mol) and DBU (0.00729 mol) were dissolved in 35 mL of dichloromethane. MBC (40.0 g, 0.160 mol) ground into fine powder was added to the above solution. The reaction lasted 20 min under nitrogen protection at 35 °C. At the end of the reaction, 2 drops of benzyl alcohol was added to terminate the reaction. Another 20 mL of dichloromethane was added to dilute the viscous polymer solution. The polymer was purified by pouring into freezing-cold ether and then filtered to separate the white solid of mPEG−PBC (52.9 g, yield 90.7%, conversion rate 81.2%). As for synthesis of polymers of

DOI: 10.1021/bm501847u
Biomacromolecules XXXX, XXX, XXX−XXX

different degrees of polymerization (DP), multiple amounts of monomer MBC were added into the polymerization reaction.

Synthesis of Poly(ethylene glycol)-block-poly(2-methyl-2-carboxyl-propylene carbonate) (mPEG–PCC). mPEG–PBC (45.4 g) was dissolved in dichloromethane/THF (1:1). Palladium on charcoal (2.25 g, 10%, Pd/C) was added into the mixed solution. The flask was purged with nitrogen twice then exchanged with hydrogen using a balloon. The reaction was carried out for 24 h with stirring at 40 °C. At the end of the reaction, Pd/C was completely removed by filtration, and the liquid was concentrated under vacuum. The remaining mixture was precipitated with cold ether. The resulting semisolid product was put under vacuum over a period to give the final mPEG–PCC (31.7 g, yield 90.7%).

Synthesis of Poly(ethylene glycol)-block-poly(2-methy-2-carboxyl-propylene carbonate-co-2-methyl-2-carboxyl-propylene carbonate)-graft-DL-α-tocopherol (mPEG–PCC–VE). mPEG–PCC (30.9 g) was dissolved in 150 mL of thionyl chloride and a drop of DMF was added as catalyst. The solvent was refluxed at 50 °C overnight. At the end of the reaction, the solvent was evaporated under vacuum. Toluene was used to dissolve the residue, and the excess of thionyl chloride was completely removed under vacuum. The resultant solid crude acid chlorides were taken directly to the next reaction. Dichloromethane (300 mL) was added to the above acid product. The mixture was stirred and cooled to 0 °C. TEA (14.1 mL, 0.103 mol) and vitamin E (23.1 g, 0.0515 mol) were dissolved in another 100 mL of dichloromethane. The mixture was added dropwise to the acid chorides solution at a slow speed. After 1 h in an ice–water bath, the solution was allowed to warm to room temperature for another 72 h. At the end of the reaction, the solvent was evaporated and extracted with dichloromethane twice. Finally, the organic layer was washed with 1 mol/L HCl three times to fully revive the carboxyl groups from acid chorides. The organic layer was given one more water wash and dried with anhydrous sodium sulfate. The final solution was concentrated under vacuum and purified by pouring into cold ether two times to obtain mPEG–PCC–VE (20.4 g, yield 55.8%).

Nuclear Magnetic Resonance (NMR). ^{1}H NMR spectra were recorded on a Bruker AVANCE III HD instrument equipped with a 400 MHz magnetic field. The proton signals of mPEG–PCC and mPEG–PCC–VE were acquired in DMSO-d_6 solution; the other products were measured in $CDCl_3$ solution.

Fourier Transform Infrared Spectroscopy (FT-IR). The chemical structures and changes of functional groups were examined by FT-IR. The polymer samples were heated to melt by an infrared generator, spread in spectroscopic grade KBr matrix by grinding, and then compressed into disks. MBC was mixed with KBr directly. Spectra were recorded by Bruker IFS 55 infrared spectrometer in the range of 400 to 4000 cm^{-1} wavenumber range. FT-IR spectra are displayed in the Supporting Information.

Gel Permeation Chromatography (GPC). Molecular weight distribution was measured by gel permeation chromatography using a Waters GPC system equipped with a GPC column (Waters Styragel HT 3 THF), THF served as both solvent and eluent at a flow rate of 1 mL/min. Calibration curve was derived from a series of narrow polystyrene standards (580–20000 g/mol).

Differential Scanning Calorimetry (DSC). The thermal properties of synthesized polymers were analyzed by DSC (Mettler Toledo DSC-1). Accurately weighed samples were sealed in an aluminum pan. Under nitrogen atmosphere, the pan was cooled to −50 °C then heated to 100 °C at a 5 °C/min heating rate. For tacrolimus and micelles, temperature was set from −50 to 200 °C at a rate of 5 °C/min. DSC results are displayed in the Supporting Information.

Critical Micelle Concentration (CMC). The CMC of mPEG–PCC–VE was determined by using pyrene as a hydrophobic fluorescent probe. Pyrene in acetone (6.0×10^{-6} M) was added in a volumetric flask. Acetone was evaporated under nitrogen airflow, and then 10 mL aliquots of polymer solution in a range of concentrations (10^{-2} to 10^{-9} g/mL) were added into the flask making the final concentration of pyrene 6.0×10^{-7} M. The samples are equilibrated in a shaker in the dark for 24 h. The excitation spectra were scanned on a Spectra Max M3 (Molecular Devices LLC, USA) at wavelengths from 300 to 380 nm, with an emission wavelength of 390 nm. At last, the intensity ratio (I_{340}/I_{336}) versus the logarithm of the polymer concentration was plotted. The CMC result is displayed in the Supporting Information.

Preparation of Polymeric Micelles. Tacrolimus and mPEG–PCC–VE were codissolved in THF and stirred for 15 min to form a homogeneous organic phase. Tacrolimus was incorporated into polymeric nanomicelles by a simple solvent evaporation method. The organic phase was injected into distilled water, and the mixture was agitated on a magnetic stirrer at a speed of 400 rpm for 12 h to evaporate THF thoroughly. Subsequently, the micelle solution was centrifuged (13000 rpm, 10 min) to remove the unloaded drug. The formulation was screened for the optimum by central composite design. The drug loading property was evaluated by drug loading efficiency and drug loading content.

Drug Loading Efficiency (DLE) and Drug Loading Content (DLC). To determine DLE and DLC, 500 μL of drug loaded micelles was diluted with 1000 μL of methyl cyanide. The solution was centrifuged (13000 rpm, 10 min) before being transferred to ultra high performance liquid chromatography (Waters ACQUITY UPLC). The mobile phase consisting of acetonitrile and redistilled water (67:33, v/v) is delivered at a flow rate of 1 mL/min, using a Kromasil-100-5C8 column (150 mm × 4.6 mm) at a column temperature of 50 °C. The TUV Detector was kept at 225 nm wavelength. The DLE and DLC were calculated by the following equations:

$$\mathrm{DLE}(\%) = \frac{M_{\mathrm{LD}}}{M_{\mathrm{D}}} \times 100\%$$

where M_{LD} stands for the amount of the loaded drug after centrifugation determined by UPLC and M_{D} is the amount of drug before centrifugation determined by UPLC.

$$\mathrm{DLC}(\%) = \frac{M_{\mathrm{FDD}}}{M_{\mathrm{FDMi}}} \times 100\%$$

where M_{FDD} means the weight of drug in freeze-dried drug loaded micelles determined by UPLC and M_{FDMi} is the weight of freeze-dried drug loaded micelles.

Size and Morphology. The particle size and polydispersity index (PDI) of the resulting micelles were measured by a Malvern Instruments Zetasizer (Nano ZS, Malvern).

Transmission electron microscopy (TEM) measurements were conducted on a JEM-2100s instrument with the accelerating voltage of 200 kV at up to 30000 magnifications. Micelles were stained by 2.0% (w/v) phosphotungstic acid for 3 min on a copper grid stabilized with carbon support film.

Central Composite Design (CCD). The formulation of the polymeric micelles was optimized by central composite design-response surface method (CCD-RSM). The aim was to investigate the influence of the THF and mPEG–PCC–VE on the resultant micelles. According to the preliminary test, the volume of THF was designed from 417.2 to 982.8 mL and the amount mPEG–PCC-VE was from 49.3 mg to 190.7 mg. The three evaluation parameters were particle size, drug loading efficiency (DLE), and drug loading content (DLC). Fitting parameters of multivariate linear regression were obtained by Design and Expert 8.0.6. Experimental data was analyzed by this software.

X-ray Diffraction (XRD) Analysis. The nanomicelles were lyophilized, and then samples were sent to XRD and DSC analysis, taking tacrolimus and mPEG–PCC–VE as controls. The X-ray powder diffraction patterns were recorded on a DX-2700 X-ray diffraction instrument (Dandong, Liaoning Province, China) at 40 kV and 30 mA. XRD results are displayed in the Supporting Information.

Stability Study. The micelles were subjected to the long-term stability study and physical stability study. In the long term stability study, micelle solution was kept at room temperature without special shading or seal handling. Samples were taken for analysis at 0, 15, and 30 days. Physical stability was carried out in a 37 ± 2 °C shaker for 30 h. Changes in particle size, polydispersity, and drug loading content were chosen to evaluate the stability of micelles. The size and PDI

DOI: 10.1021/bm501847u
Biomacromolecules XXXX, XXX, XXX–XXX

Scheme 1. Synthesis of mPEG−PCC−VE[a]

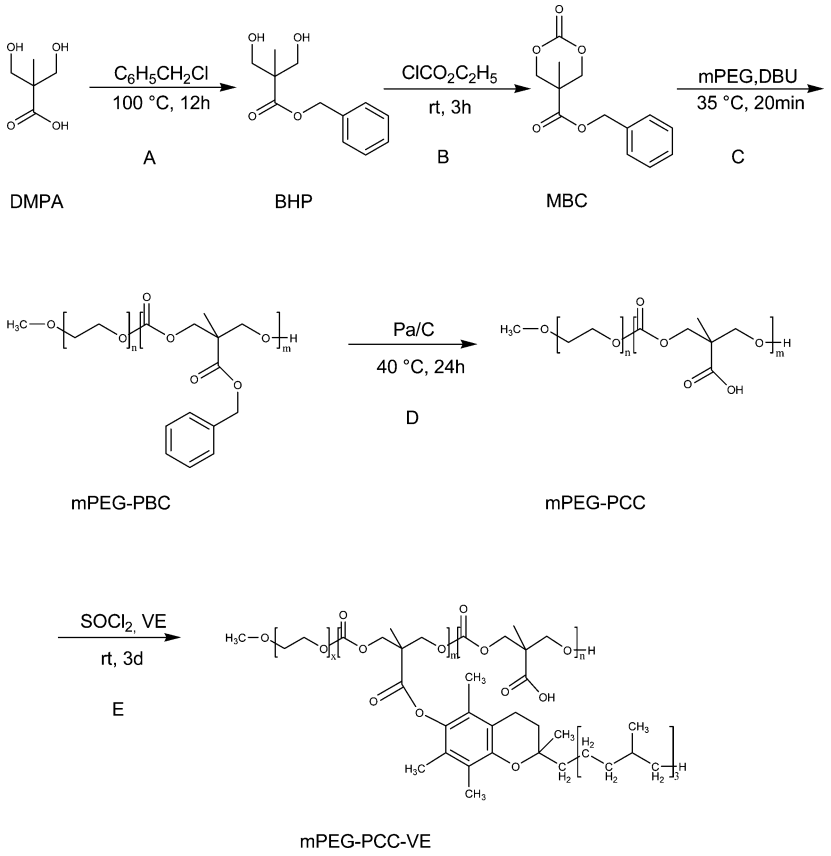

[a]Conditions: (A) DMF, 100 °C, 12 h; (B) $ClCO_2C_2H_5$, THF, rt, 3 h; (C) DBU, CH_2Cl_2, 35 °C, 20 min; (D) Pa/C, THF/CH_2Cl_2 (1:1), 40 °C, 24 h; (E) $SOCl_2$, DMF, rt, 3 d.

were measured before centrifugation of samples, and DLC was measured after centrifugation to remove the leakage of drugs. The results of the stability study are detailed in the Supporting Information.

In Vitro Drug Release. Micelle solution (1 mL) in a dialysis bag (MWCO = 10000) was suspended in 30 mL of simulated gastric fluid (SGF, pH = 1.2) or 30 mL of phosphate buffer solution (PBS, pH 6.8 and 7.4). The *in vitro* release was conducted under the sink condition (adding 0.1% tween 80). The samples were incubated in a 37 °C shaker; 3 mL of the release medium was withdrawn and replaced with 3 mL of fresh SGF or PBS at specified intervals. Tacrolimus was analyzed by UPLC as mentioned above. The SGF and PBS in this research were prepared according to the formulation of Chinese Pharmacopoeia.

pH-Dependent Swelling Profile. Similar to the preparation of nanomicelles in distilled water, the organic phase was injected into different pH media (pH 1.2, 8.0) and water. The solvent was evaporated to observe the self-assembly outcomes.

The variation in micelle size versus time (0−31 h) in different PBS solutions (pH 1.2, 4.5, 6.0, 6.8, 7.8) was studied. After storage at room temperature for 72 h, the ultimate state of pH-sensitive micelles in different PBS solutions was determined.

In Situ Single-Pass Intestinal Perfusion. All animals investigated were executed according to the Guidelines for the Care and Use of Laboratory Animals Approved by the Ethics Committee of Animal Experimentation of Shenyang Pharmaceutical University. Sprague−Dawley rats weighting 230−250 g fasted overnight with free access to water were anaesthetized with 20% urethane (1 g/kg) by intraperitoneal injection. The rats were operated on under a warm infrared lamp to maintain body temperature. The abdominal area was sterilized with 75% ethanol, and the intestine was exposed by making a 4 cm incision along the midline. The isolated segments of duodenum, jejunum, ileum, and colon were cannulated longitudinally at both the proximal and distal ends. The intestinal segments measured about 10 cm at length with glass cannulas attached to tygon tubing system and secured by sutures. Before the perfusion experiment, the intestinal segments were gently washed with warm saline solution with a syringe and then purged with 30 μg/mL fresh tacrolimus-loaded micellar dispersion (2.25 mL of tacrolimus micellar solution was diluted into 150 mL of K-R buffer, which consisted of 7.8 g of NaCl, 0.35 g of KCl, 1.37 g of $NaHCO_3$, 0.32 g of NaH_2PO_3, 0.02 g of $MgCl_2$, 1.4 g of glucose, and 0.32 g of $CaCl_2$ per 1000 mL). Saline-wetted gauzes were used to prevent the rat's body from dehydrating. The temperature-controlled inlet perfusate (37 °C) was furnished at speed of 0.2 mL/min throughout a peristaltic pump. The outflowing perfusate was collected at 15 min intervals continuously up to 90 min (n = 6). The difference in weight between inlet and outlet perfusate was recorded. At the end of the experiment, the rats were executed. The length and radius of experimental intestine was measured. The concentration of drug in the donor and receptor was determined by UPLC. The absorption rate (K_a) and apparent permeability (P_{app}) were calculated by the following equations:

$$K_a = \left(1 - \frac{C_{out}}{C_{in}}\frac{V_{out}}{V_{in}}\right)\frac{v}{V}$$

$$P_{app} = \frac{-v \ln\left(\frac{C_{out}}{C_{in}}\frac{V_{out}}{V_{in}}\right)}{2\pi r l}$$

where C_{out} is the concentration of tacrolimus in the outlet perfusate, C_{in} is the concentration of tacrolimus in inlet perfusate, V_{out} is the volume of perfusate collected in the receptor tube, V_{in} is the volume of perfusate pumped from the donor flask, l is the length of the isolated intestine for perfusion, r is the radius of the intestinal segment, and v is the flow rate of perfusion.

DOI: 10.1021/bm501847u
Biomacromolecules XXXX, XXX, XXX−XXX

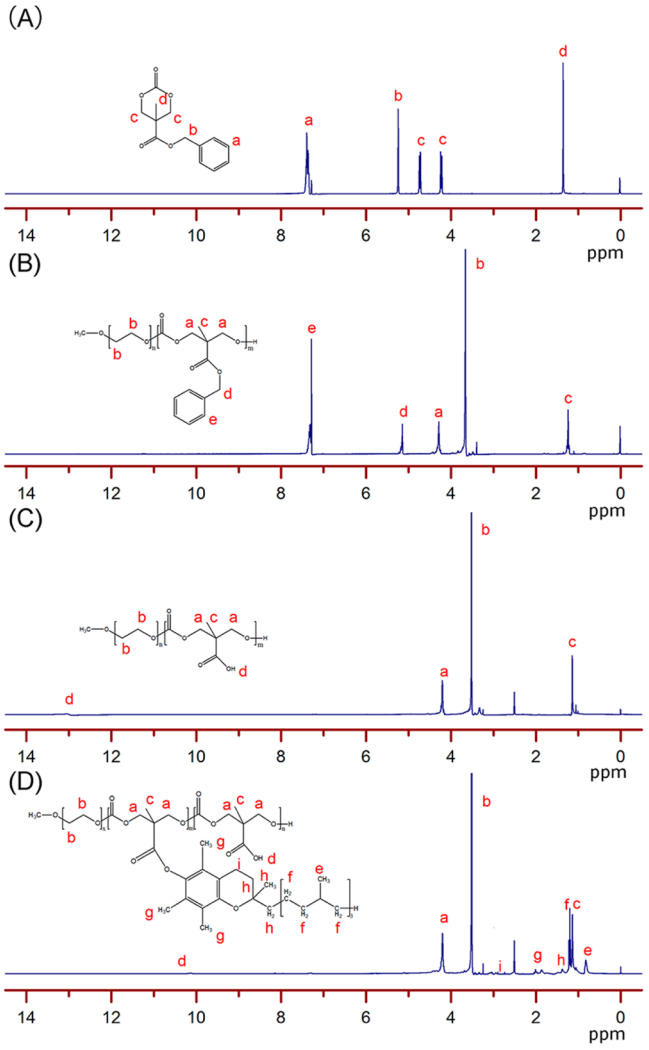

Figure 2. ^{1}H NMR of the monomer and polymers: (A) MBC; (B) mPEG$_{113}$−PBC$_{32}$; (C) mPEG$_{113}$−PCC$_{32}$; (D) mPEG$_{113}$−PCC$_{32}$−VE$_4$.

Biodistribution of Coumarin-6 Labeled Nanomicelles in the Gastrointestinal Tract. Micelles encapsulating coumarin-6 were orally administrated to Sprague−Dawley rats. After 40 min, the rat was sacrificed. Isolated by incision and frozen in OTC, the everted segments of duodenum, jejunum, ileum, and colon were sliced at 7 μm intervals. The intestinal tissue was incubated with 4% paraformaldehyde and washed three times with cold PBS (pH 7.4). Then the tissue slide was incubated with triton (0.5%) and subsequently washed with PBS. After staining with DAPI and rhodamine phalloidin for visualization of cell nuclei (blue) and cytoskeleton (red), the enterocyte was observed by confocal laser scanning microscopy (LSM 710 NLO).

Inhibition of P-gp Efflux Tests. P-pg inhibitory effect of mPEG−PCC−VE was evaluated by the absorption of tacrolimus micelles in the presence and absence of standard P-gp inhibitor verapamil. The ileum of SD rats was rinsed with 37 °C KR buffer and everted with a glass rod. The everted intestine was cut to about 100 mg rings and placed in a 24-well plate. The intestinal rings were washed with 1 mL of KR buffer twice and were incubated in KR solution with or without verapamil (100 mg/mL) for 45 min at 37 °C. Afterward, the incubation media was removed, and 1 mL of a micellar solution of tacrolimus (100 μg/mL) was added, followed by incubation for 45 min. The intestinal segments were finally washed and homogenized. Tacrolimus extracted from the intestinal homogenate was analyzed by HPLC. The tacrolimus solution group underwent the same process as described above.

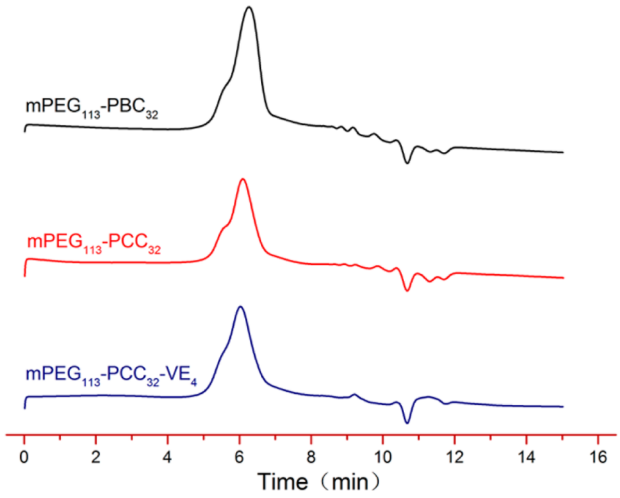

Figure 3. GPC measurements of mPEG$_{113}$−PBC$_{32}$, mPEG$_{113}$−PCC$_{32}$, and mPEG$_{113}$−PCC$_{32}$−VE$_4$.

Pharmacokinetic Study. The absorption of tacrolimus was systematically evaluated for oral administration. Ten rats in fasted state were randomly divided into two groups. Two groups of rats were fed with tacrolimus-solution (15 mg/kg) and tacrolimus-nanomicelle (15 mg/kg); 400 μL of blood was collected at specific time intervals. The blood concentration during 12 h after administration was determined by UPLC−MS/MS (Waters ACQUITY UPLC/tandem quadrupole detector). The blood samples were stored in a −20 °C freezer until analysis. The gradient elution of UPLC, MS conditions, and sample processing have been reported in our previous work.[39]

Briefly, analyses were acquired by an ACQUITY UPLC system (Waters Co). An ACQUITY UPLC BEH C18 column (50 mm × 2.1 mm, 1.7 μm) was used, while mobile phase was composed of acetonitrile and water premixed with 0.1% formic acid. Gradient elution program began at 15% water for 0.2 min, and then changed linearly to 10% water (0.2−0.5 min), then to 5% water (0.5−2.8 min),and at last changed to the initial conditions (2.8−3.0 min). The column temperature was set at 50 °C with 0.2 mL/min flow rate. The injection volume was 10 μL.

The ionization source conditions were as follows: source temperature of 120 °C and desolvation temperature of 350 °C; the cone voltage of 50 V and capillary voltage of 3.2 kV; the cone gas flow rates of 50 L/h and desolvation gas flow rates of 500 L/h; collision energy of 34 and 19 V for tacrolimus and glibenclamide (I.S.), respectively. Quantification was carried out by multiple reaction monitoring with transitions from m/z 826.3 to 616.5 for tacrolimus and m/z 494.0 to 352.0 for glibenclamide (I.S.). The scan time was set at 0.2 s per transition.

The mixture of dichloromethane and n-hexane (1:1, 2 mL) and I.S. solution (100 μL, 20 μg/mL) was added to the 100 μL blood sample. After vortex for 3 min and centrifugation for 10 min (3500 rpm), the organic layer was separated and evaporated completely at 35 °C under

Table 1. Molecular Weight Characterization of Polymers in Reactions

polymer	M_n, NMR	M_n, GPC	M_w, GPC	M_p, GPC	M_Z, GPC	M_w/M_n	yield (%)
mPEG$_{113}$−PBC$_{32}$	12250	10323	11564	11094	12915	1.12	90.8
mPEG$_{113}$−PCC$_{32}$	9542	10491	12237	11989	13753	1.12	89.5
mPEG$_{113}$−PCC$_{32}$−VE$_4$	12646	10660	12613	12799	14208	1.13	44.2

DOI: 10.1021/bm501847u
Biomacromolecules XXXX, XXX, XXX−XXX

Table 2. Characterizations and Comparison of $mPEG_{113}$−PCC_8−VE_2, $mPEG_{113}$−PCC_{16}−VE_4, $mPEG_{113}$−PCC_{32}−VE_4, and $mPEG_{113}$−PCC_{64}−VE_4

polymers	DP, NMR	VE, NMR	M_n, NMR	M_n, GPC	M_w, GPC	M_P, GPC	M_Z, GPC	M_w/M_n	D_h (nm)	PDI	DLE (%)	DLC (%)
$mPEG_{113}$−PCC_8−VE_2	9.3	2.1	7362	9706	11033	9790	12470	1.13	179.1	0.438	3.0	0.8
$mPEG_{113}$−PCC_{16}−VE_4	14.7	3.6	8907	8812	11244	9831	13522	1.20	91.9	0.623	3.9	1.0
$mPEG_{113}$−PCC_{32}−VE_4	35.5	4.6	12646	10491	12237	11989	13753	1.12	89.7	0.186	81.1	19.7
$mPEG_{113}$−PCC_{64}−VE_4	63.5	4.1	16933	18550	18773	17333	19001	1.13	107.2	0.091	5.9	1.6

gentle nitrogen airflow. The residue was dissolved in 100 μL of mobile phase followed by vortex-mixing and centrifugation (13000 rpm, 10 min). The resultant supernatant was transferred to UPLC-MS for analysis.

Statistical Analysis. The statistical analysis was accomplished by student's t test for experiments, while $P < 0.1$ was deemed statistical difference.

RESULTS

Synthesis and Characterization. According to the synthetic route shown in Scheme 1, the carboxyl groups of DMPA were first protected by benzyl chloride instead of commonly used benzyl bromide. The yield of BHP turned out to be 73.11%, higher than with protection by the benzyl bromide method.[40] MBC was obtained from ring-closing of BHP, subsequently subjected to organocatalytic ring open polymerization (ROP) initiated by mPEG5000. mPEG−PCC resulted from deprotection of the benzyl group via hydrogenolysis. Finally, a portion of reactive pendant carboxyl groups of mPEG−PCC was conjugated to vitamin E via postpolymerization modification. ^{1}H NMR spectrum report of $mPEG_{113}$−PCC_{32}−VE_4 is given in Supporting Information (Figure 1).

The postpolymerization modification provides two functional groups and high-yielding polymers. Using thionyl chloride in conjugation with VE could circumvent the limitation of low esterification efficiency and result in the maintenance of carboxyl groups with the hydrolysis of unreacted acyl chlorides. The thionyl chloride method prohibited the cross-linking between carboxyl and terminal OH groups and prevented the carboxyl from connection with conventional condensation agents (DCC and EDC, for instance) as well. The synthesized mPEG−PCC−VE exhibited narrow dispersion of molecular weight.

From ^{1}H NMR spectra of mPEG−PBC (Figure 2B), peaks at δ 4.7 (d, 2H) and 4.2 (d, 2H) of monomer MBC (Figure 2A) disappeared, and a new peak emerged at δ 4.3, demonstrating the success of ROP. The repeated CH_2 at δ 4.3 in polycarbonates was used to estimate the DP and molecular weight by comparing with CH_2 of mPEG at δ 3.7. The polymerization was well-tailored to generate polymers of different DP (ranging from 8 to 64) with conversion rate up to 81.2%. The pendant benzyl protection was completely removed by hydrogenation as demonstrated by disappearance of the peak at δ 7.3 (phenyl ring) and appearance of the peak at δ 13.1 (the carboxyl group) (Figure 2C). The conjugation of vitamin E was confirmed and quantified by the peak at δ 0.8, belonging to the methyl groups of the aliphatic chain on vitamin E (Figure 2D).

Molecular weights of polymers were determined by ^{1}H NMR and GPC as described in Table 1. M_n of $mPEG_{113}$−PBC_{32} measured by ^{1}H NMR decreases after removal of the benzyl groups ($mPEG_{113}$−PCC_{32}). M_n of $mPEG_{113}$−PCC_{32}−VE_4 showed an increasing tendency compared with $mPEG_{113}$−PCC_{32} confirming the incorporation of VE groups. GPC curves (Figure 3) of $mPEG_{113}$−PBC_{32}, $mPEG_{113}$−PCC_{32}, and $mPEG_{113}$−PCC_{32}−VE_4 all showed a monomodal symmetric distribution with PDI (M_w/M_n) below 1.13 (listed in Table 1), demonstrating a well-controlled polymerization and narrow dispersion of molecular weights. The GPC measurement suggested that M_n of $mPEG_{113}$−PCC_{32} might be higher than that of $mPEG_{113}$−PBC_{32} contrary to our speculation. This phenomenon might be caused by the addition of abundant carboxyl, which resulted in shorter retention in our GPC column. The molecular weights were almost consistent with the theoretical values. Therefore, $mPEG_{113}$−PCC_{32}−VE_4 was successfully synthesized and characterized.

Comparison between Different Polymers. The physicochemical properties of a series of polymers and with different DP are compared in Table 2. These polymers had the same hydrophilic chains of mPEG5000 but connected with the different lengths of hydrophobic polycarbonate chains. The four kinds of the micelles were prepared by the same method, with identical weight of mPEG−PCC−VE and drug. Small PDI (M_w/M_n) measured by GPC revealed the narrow dispersion of all the polymers. Both $mPEG_{113}$−PCC_8−VE_2 and $mPEG_{113}$−PCC_{16}−VE_4 could self-assemble to micelles with PDI > 0.4 and DLE < 5%. $mPEG_{113}$−PCC_{32}−VE_4 and $mPEG_{113}$−PCC_{64}−VE_4 were able to form homogeneous sized micelles with PDI < 0.2, but $mPEG_{113}$−PCC_{32}−VE_4 exhibited more than 10 times higher DLE (81.1%) and DLC (19.7%) than $mPEG_{113}$−PCC_{64}−VE_4. This implied that the balance between amphiphilic chains profoundly influenced the formation of micelles. As a result, $mPEG_{113}$−PCC_{32}−VE_4 was selected to load tacrolimus in subsequent experiments.

We explored whether conjugation to vitamin E improved the drug loading properties of the polymers (Table 3). After attaching five vitamin E groups to the polycarbonate chain, $mPEG_{113}$−PCC_{32}−VE_4 possessed much higher DLE and DLC than the others without vitamin E attachment. Therefore, a vitamin E modified brush-like hydrophobic chain greatly increased the drug loading efficiency. Moreover, the particle sizes were ranked as follows: mPEG−PCC > drug loaded mPEG−PCC−VE > mPEG−PCC−VE > mPEG−PBC. The size of carboxylic functionalized mPEG−PCC was the largest among all polymers. Compared with mPEG−PCC, conjugation to vitamin E led to a decrease in particle size. That is to say,

Table 3. Characterization of Micelles Self-Assembled from Different Polymers and Comparison of Their Drug Loading Properties

polymers	size (nm)	PDI	ζ	DLE (%)	DLC (%)
$mPEG_{113}$−PBC_{32}	100.3	0.23	−1.81	9.4	4.5
$mPEG_{113}$−PCC_{32}	138.9	0.09	−4.37	38.6	8.9
$mPEG_{113}$−PCC_{32}-VE_4	111.4	0.23	−4.26	75.0	21.3
drug-loaded $mPEG_{113}$−PCC_{32}−VE_4	126.4	0.14	0.33		

DOI: 10.1021/bm501847u
Biomacromolecules XXXX, XXX, XXX−XXX

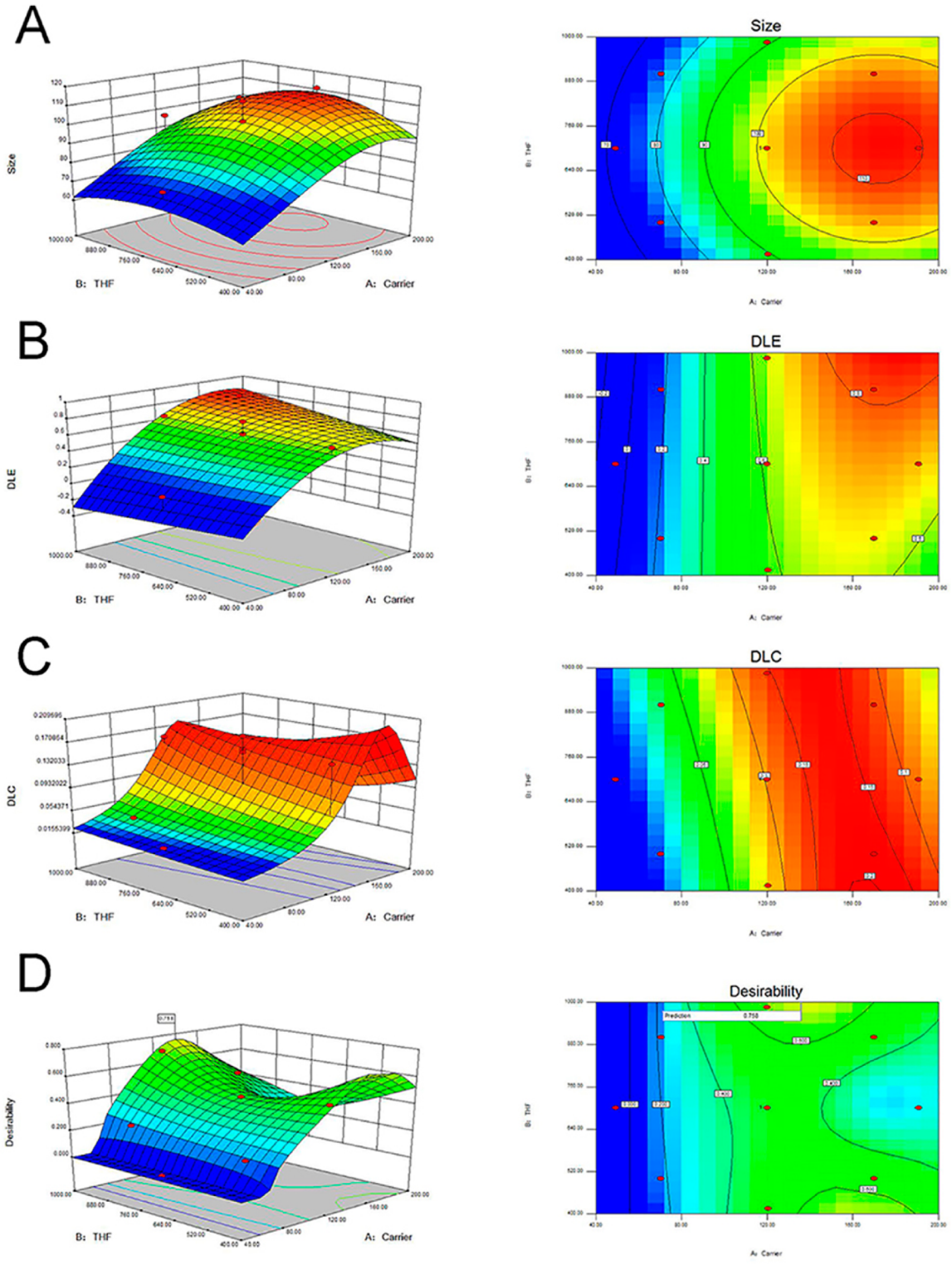

Figure 4. Three-dimensional response surface and contour plot spreading on (A) size, (B) DLE, (C) DLC, and (D) desirability.

although the molecular weight of mPEG−PCC−VE was larger than that of mPEG−PCC, the size of mPEG−PCC−VE assemblies was smaller. When tacrolimus was loaded, the increase in drug-loaded micelle volume can be observed in contrast to that of mPEG−PCC−VE. TEM images of these different micelles are displayed in Figure 5.

Central Composite Design. The response surfaces of CCD are illustrated in Figure 4. The response surface in Figure 4A shows the effect of carrier (variable A) and THF (variable B) on size. Variable B has little effect on the size of micelles. With variable A amount from 40 to 200 mg, particle size increased from about 90 to 150 nm. Figure 4B displays the effect of variables on DLE. The maximum of both A and B led to the highest DLE. An obvious ridge spread on the surface of DLC (Figure 4C) along the change of A, indicating that certain range of A (120−160 mg) resulted in relatively high DLC. Taking the

DOI: 10.1021/bm501847u
Biomacromolecules XXXX, XXX, XXX−XXX

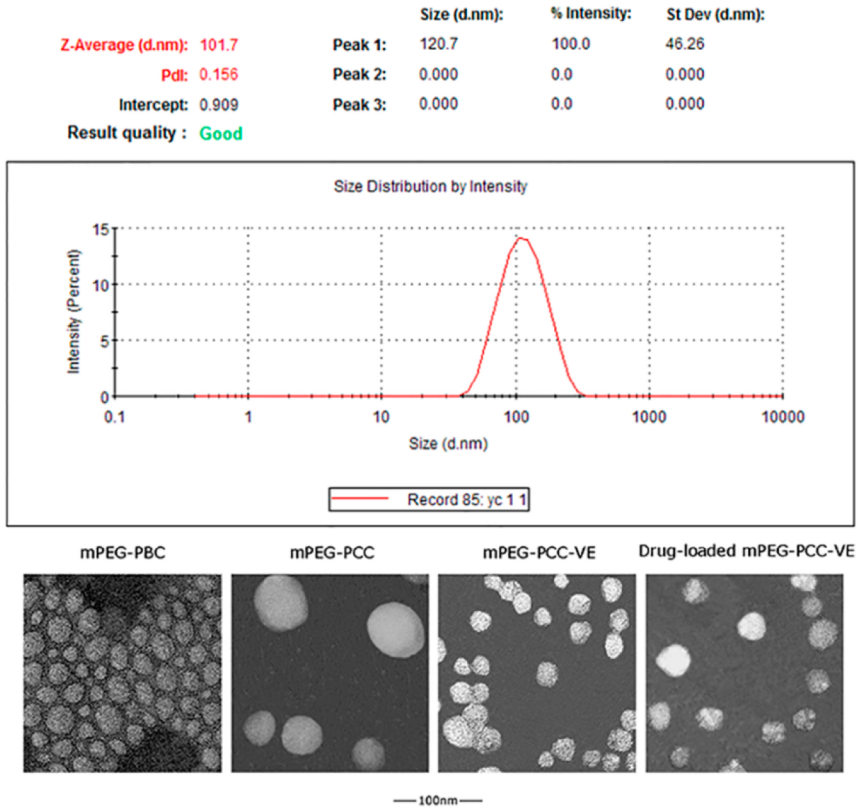

Figure 5. Size and size distribution of drug loaded $mPEG_{113}$–PCC_{32}–VE_4 and morphology of blank $mPEG_{113}$–PBC_{32}, $mPEG_{113}$–PCC_{32}, $mPEG_{113}$–PCC_{32}–VE_4 and tacrolimus loaded $mPEG_{113}$–PCC_{32}–VE_4 micelles.

result of the three responses into account, the desirability versus A and B was given by Figure 7D. The model was verified by prediction, indicating a desirable predictive effect and relatively high reliability. The optimized micelle formulation given by CCD consisted of 135.9 mg of $mPEG_{113}$–PCC_{32}–VE_4 and 980.0 μL of THF with size of 101.7 ± 19.4 nm, DLE of 80.2% ± 7.3% and DLC of 21.2% ± 2.7% with tacrolimus concentration of 7.2 mg/mL. The detailed description is available in Supporting Information (Tables 1–5).

Characterizations of Micelles. Dynamic light scattering (DLS) focused on the evaluation of the size and size distribution of tacrolimus loaded micelles. DLS (Figure 5) results indicated a size of 101.7 nm and PDI of 0.156 agreeing well with TEM. TEM images directly visualized the spherical structures of micelles, indicating that the amphiphilic polymers yielded spherical micelle.

pH-Sensitive Properties of $mPEG_{113}$–PCC_{32}–VE_4. We studied the pH-dependent swelling profile of $mPEG_{113}$–PCC_{32}–VE_4 (Figure 6A). At pH 6.8 and pH 7.4, the diameter of micelles increased rapidly and then came to a plateau about 230 nm with the swelling ratio of 2.5. At pH 1.2 and 4.5, the particle size remained at the initial level for 31 h without significant variations. Micelles at pH 6.0 were at an intermediate level, suggesting that pH 6.0 may be around the critical value to trigger the pH-dependent swelling behavior. Micelles in pH 1.2 and 4.5 shrank to about 70 nm lower than the size of the control prepared in water. These four micellar solutions were stored at room temperature for 3 days. Predictable sediment of tacrolimus caused by the drug leakage in disassembled micelles was observed in pH 6.0, 6.8, and 7.4, and the supernatant became completely transparent. By contrast, micelles in pH 1.2 and 4.5 remained their light blue opalescence and no insoluble drugs appeared. The detailed description and photograph are available in Supporting Information.

The pH-dependent profile was further confirmed by *in vitro* drug release. Figure 6B showed the *in vitro* release of tacrolimus at pH 7.4, 6.8, and 1.2. In pH 7.4 PBS media, 18.9% of tacrolimus was released from the micelles over a 3 h period and 96.2% was released after 24 h. At pH 1.2, since pendant carboxyl groups were protonated, drug release was 3.4% at 3 h and 52.0% after 24 h, indicating that the pH-sensitive cores could markedly reduce the release of the loaded cargo in acidic pH. In addition, $mPEG_{113}$–PCC_{32}–VE_4 micelles efficiently prolonged the release of drug in a controlled manner in contrast with the solution group.

Biodistribution of Coumarin-6 Labeled Nanomicelles. Intestinal segments were imaged with a confocal laser scanning microscope (CLSM) to determine the epithelial cell disposition of coumarin-6 loaded micelles in the presence and absence of $mPEG_{113}$–PCC_{32}–VE_4 (Figure 7). The CLSM micrographs revealed that the absorbed coumarin-6 micelles (Figure 7A) were localized intracellularly with stronger fluorescence intensity and deeper permeation in comparison to coumarin-6 solution (Figure 7B). The results provided visual evidence that the $mPEG_{113}$–PCC_{32}–VE_4 enhances the absorption of loaded drug in all segments of the intestine. More specifically, colon was observed to have the most absorption versus duodenum, jejunum, and ileum.

***In Situ* Single-Pass Intestinal Perfusion and Inhibition of P-gp Efflux Tests.** The absorption parameter (K_a) was introduced to describe the absorption rate of drug; the permeability of the drug was evaluated by the apparent permeability coefficient (P_{app}). *In situ* single-pass perfusion (Figure 8A) showed that the ileum turned out to have the lowest K_a and P_{app},

DOI: 10.1021/bm501847u
Biomacromolecules XXXX, XXX, XXX–XXX

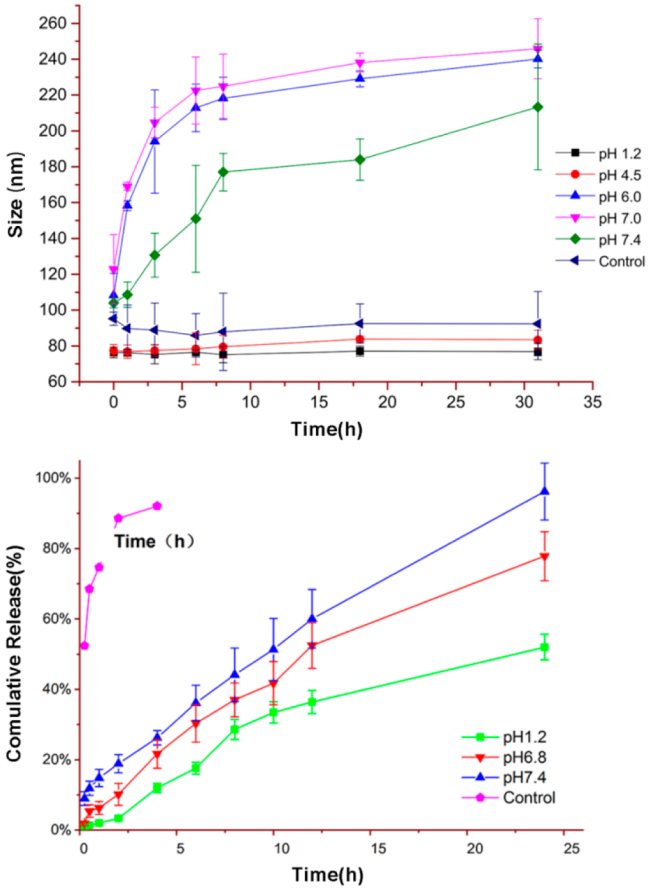

Figure 6. (A) pH-dependent swelling profile of $mPEG_{113}$–PCC_{32}–VE_4 micelles in different pH; size variations were recorded during specific time intervals. (B) *In vitro* release of tacrolimus loaded micelle in pH 1.2, pH 6.8, and pH 7.4 PBS with the control of tacrolimus solution.

possibly because the activities of P-gp increased from proximal to the distal intestine segments.[41] Colon exhibited the highest K_a and P_{app}, in an agreement with the result of biodistribution study, because colon was likely to possess a special mechanism responsible for the high absorption of tacrolimus micelles.

The presence of verapamil significantly enhanced the absorption of tacrolimus in ileum ($p < 0.1$) as illustrated in Figure 8B, confirming that tacrolimus was a potent P-gp substrate. The absorption of tacrolimus was significantly ($p < 0.01$) increased by $mPEG_{113}$–PCC_{32}–VE_4 micelles versus the solution group, which might be ascribe to two aspects. For one thing, $mPEG_{113}$–PCC_{32}–VE_4 might have an inhibitory effect on P-gp. For another, the nanoscale micelles possess more advantages over solution preparation in oral absorption. Interestingly, adding verapamil made no significant difference to the micellar group, implying that $mPEG_{113}$–PCC_{32}–VE_4 might act as verapamil did.

Pharmacokinetic Study. The blood tacrolimus concentration versus time is shown in Figure 9. The related pharmacokinetic parameters were displayed in Table 4. At 0.3 h postadministration, the group orally administrated tacrolimus solution exhibited rapid absorption (T_{max} = 0.33 h), whereas T_{max} of tacrolimus-nanomicelle was 1.7 h. The C_{max} and $AUC_{(0-12h)}$ of the group orally treated with tacrolimus solution were 149.2 ± 71.7 ng/mL and 320.8 ± 121.5 ng/(mL·h), respectively. In contrast, the C_{max} and $AUC_{(0-12h)}$ of micelles

Table 4. Pharmacokinetic Parameters of Tacrolimus in Rats after Oral Administration[a]

	tacrolimus-sol	tacrolimus-nanomicelle
dose (mg/kg)	15.0	15.0
$AUC_{(0-12h)}$	320.8 ± 121.5	1926.1 ± 533.0
$t_{1/2}$ (h)	5.9 ± 4.4	2.3 ± 1.1
T_{max} (h)	0.33 ± 0.17	1.70 ± 0.76
C_{max} (ng/mL)	149.2 ± 71.7	467.4 ± 94.8

[a]AUC, area under the blood concentration–time curve; $T_{1/2}$, terminal half-life; T_{max}, time when C_{max} is attained; C_{max}, maximum blood concentration; data are given as mean ± SD (n = 5 for each group).

were 467.4 ± 94.8 ng/mL and 1926.1 ± 533.0 ng/(mL·h) (6-fold compared with tacrolimus-sol), which is an encouraging outcome in consideration of the difficulties encountered in the oral absorption. The pharmacokinetic study demonstrated that $mPEG_{113}$–PCC_{32}–VE_4 nanomicelles developed in this study significantly enhanced intestinal absorption and oral bioavailability of tacrolimus.

DISCUSSION

Amphiphilic macromolecules form micellar architectures in aqueous solution, which are capable of loading insoluble drugs.[42] In our study, the hydrophobic core-block length is varied, and the resultant micellar properties including size, stability, and loading capacity were measured to help comprehensive understanding of the relationship between chemical composition and corresponding physical properties. To summarize, the optimal polymer structure was composed of mPEG5000 (M_n), hydrophobic polycarbonate 5000 (M_n) and 2000 (M_n) vitamin E, which spread a brush-shaped hydrophobic region.

We chose the central composite design (CCD) for formulation optimization because of its efficiency in exploring two-factor interactions and detecting quadratic effects. With fewer experimental conditions than full factorial designs, CCD gives output of response surfaces for exploring the significant amount of formula in micelle preparation.[43] CCD herein aided finding the maximized drug loading formulation. We could conclude from the response surfaces that the more $mPEG_{113}$–PCC_{32}–VE_4 added, the higher DLE can be achieved. However, DLC did not show an identical trend. When DLE peak value was attained, adding more $mPEG_{113}$–PCC_{32}–VE_4 remarkably decreased DLC value. Therefore, a proper ratio of water phase, organic phase, and surfactant was critical to maximize drug loading and minimize particle size.

Some pH-sensitive micelles for oral administration were prepared and stored only in acidic pH region. Our newly developed pH-sensitive polymers were able to remain stable micelle structures in water for a month (stability study is displayed in Supporting Information Table 6), which was superior to previous ones.[14,15] These self-assemblies in water are mainly driven by hydrophobic attractions among vitamin E segments, suppressing the electrostatic repulsions between charged carboxyl groups. When pH is increased, the ionized carboxyl groups favored the dissociation of the structure. As a result, repulsion-driven forces might dominate the reversal of self-assembly.

pH-dependent swelling and drug release were affected by solution variables, such as pH and solution ionic strength.[44] For pH near or above pK_a, deprotonation was favored by the acid–base equilibrium. When repulsion among charged

DOI: 10.1021/bm501847u
Biomacromolecules XXXX, XXX, XXX–XXX

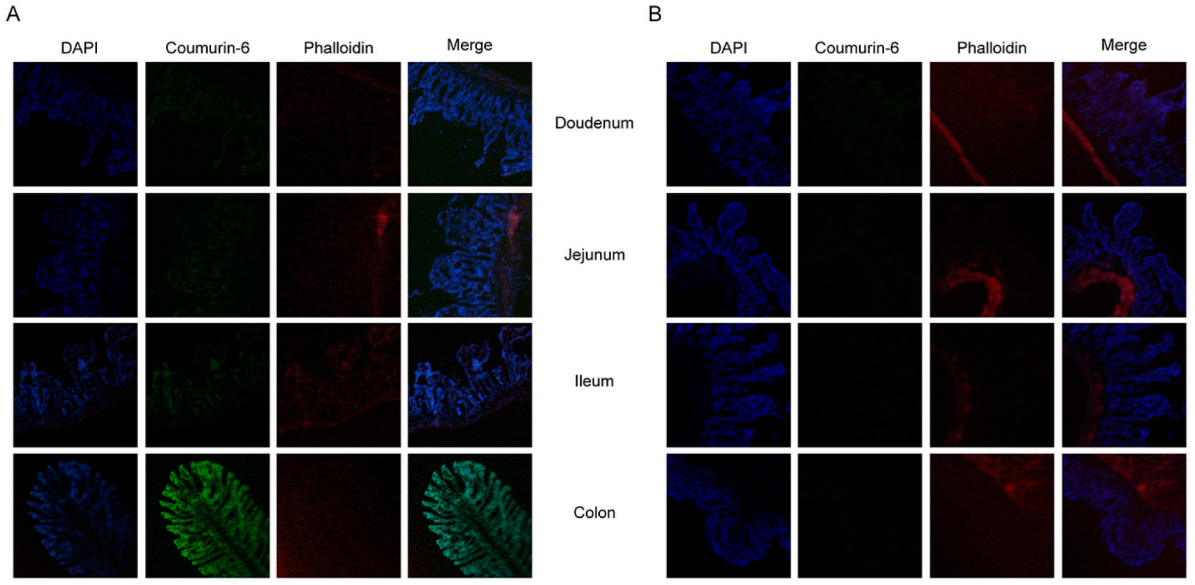

Figure 7. Intestinal segment fluorescence of (A) SD rats treated with nanomicelles encapsulating coumarin-6 (green fluorescence) and (B) SD rats treated with coumarin-6 solution. DAPI (blue) was used to capture the nucleus of the histological sections. Rhodamine phalloidin (red) was used to counterstain the cytoskeleton.

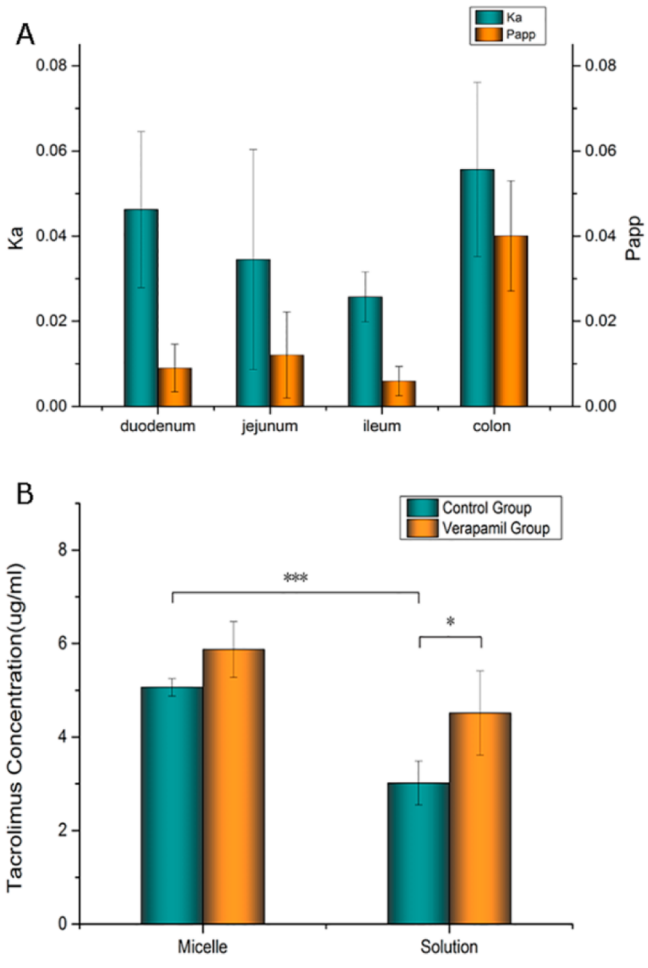

Figure 8. (A) *In situ* single-pass perfusion, K_a and P_{app} of duodenum, jejunum, ileum, and colon (n = 6 for each group). (B) The inhibition of P-gp efflux test in ileum segment. Verapamil was used as standard P-gp inhibitor. The groups treated without verapamil were used as controls (*p < 0.1; ***p < 0.01).

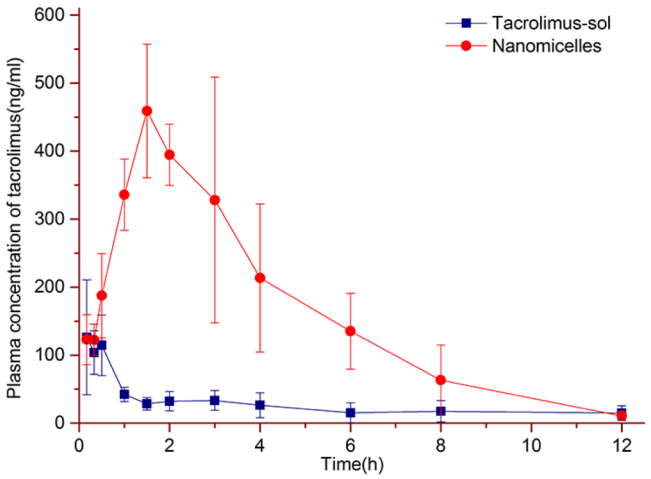

Figure 9. Blood tacrolimus level versus time after oral administration of tacrolimus loaded nanomicelles and solution preparations to SD rats.

carboxyl became sufficiently strong, it caused the hydrophobic chains to reduce electrostatic interactions by swelling, at the cost of decreasing the hydrophobic attraction. The formation of the micelles will therefore be unfavorable. The ionized carboxyl is surrounded by a charged ionic atmosphere, which partially screens the carboxyl from protonation. Increasing the ionic strength by adding salts decreased the formation of protonated carboxylic acid, and apparently benefitted the swelling of micelles. The small swelling ratio of the $mPEG_{113}$–PCC_{32}–VE_4 micelles conducted a controlled release.

Oral administration features convenience, painless administration, and high compliance with patients especially those in need of chronic therapies. The intravenous-to-oral switch in chemotherapy is recommended in our recent review due to its innate patient compliance and mild sustained drug concentration in the circulation.[45] At present, more than 60% of marketed drugs are administered via the oral route,[46] but approximately 70% of new chemical entities exhibit poor

DOI: 10.1021/bm501847u
Biomacromolecules XXXX, XXX, XXX−XXX

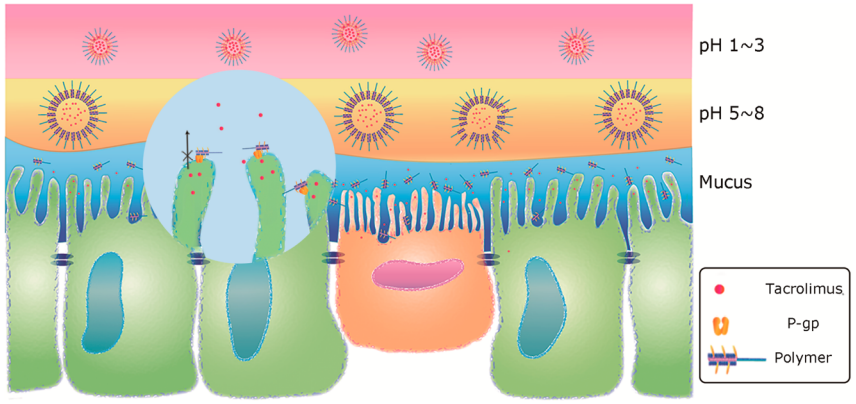

Figure 10. Illustrated mechanism of pH-sensitive oral absorption.

soluble in aqueous solution.[47] According to the Biopharmaceutics Classification System (BCS), class II drugs are characterized by poor aqueous solubility and high permeability, and poor solubility continues to be a therapeutic threshold to oral absorption.[5] Besides, drug efflux by the intestinal epithelial ATP-binding cassette transporter P-gp plays a determining role in restricting membrane permeability.[48−52]

Tacrolimus (FK506) is an immunosuppressant usually used to prevent graft rejection after organ transplantations, as well as to treat autoimmune diseases.[53,54] Tacrolimus belongs to BCS class II substances, and it is a typical cosubstrate of P-gp and cytochrome P450 (CYP) 3A enzymes. The above characteristics result in poor *in vivo* absorption of tacrolimus. However, development of an oral tacrolimus delivery system is of great significance for chronic treatment to transplant recipients. P-gp efflux should be responsible for poor oral bioavailability of tacrolimus to a great extent.[55] D-α-Tocopheryl polyethylene glycol succinate (vitamin E TPGS) was reported to serve as a P-gp inhibitor for improving the oral bioavailability due to its functional group vitamin E.[56] Similarly, in our study, the increased absorption of tacrolimus was probably because the nanocarriers have abundant vitamin E, which functioned as a P-gp inhibitor.

In this study, anionic polymers with carboxyl and vitamin E were to maintain the hydrophobic cores at stomach pH but swell to release drug at intestinal neutral pH. The nanoscale of micelles might also facilitate adhesion to mucus,[57−59] and prolong residence time in the gut by physical absorption.[60,61] In the meantime, the bioadhesion of carriers to mucosa (pH 5.0−6.5) was augmented, since the swelling micelles transform from solid to gel enhancing the *in vivo* absorption.[62] The functional vitamin E group might further facilitate the drug absorption by acting as a P-gp inhibitor to reduce drug efflux. The possible schematic diagram of nanomicelles across a pH gradient in GI track is illustrated in Figure 10.

CONCLUSIONS

A serial length of hydrophobic polycarbonate chains with functional carboxyl and VE were successfully synthesized via postpolymerization modification. We demonstrated that variations in drug loading capability were attributed to the chain length and the hydrophobic vitamin E tips. CMC of the optimal structure was extraordinarily low suggesting that the micelles were stable against dilution, which was later verified by the stability test. In the nanomicelle formulation, CCD was used to build the fitting the second-order models for manipulating size, DLE, and DLC to desirable values. The resultant micellar structure exhibited low leakage of drug in pH 1.2 release media and could overcome the drastic pH environment in stomach, subsequently conducting the controlled release of drug in the intestinal pH environment. Experiments were further performed to confirm that this drug delivery system was adequate to encapsulate drugs efficiently and transport them in the GI tract with improved oral bioavailability, as well as inhibiting the drug efflux mediated by P-gp. The novel anionic pH-responsive polymer was appropriate for delivering a variety of drugs, such as preventing gastric degradation of drug like insulin, improving loading content of cationic drugs like doxorubicin, improving bioavailability of a P-gp substrate, and specifically binding drugs with amino, forming clathrate or chelate with drugs by noncovalent binding. More work will be done to realize the control and optimization of this polymer, as well as to explore mechanism of its oral administration. Therefore, this newly developed pH-responsive polymer has the possibility to be a useful biomaterial for oral drug delivery.

ASSOCIATED CONTENT

Supporting Information

Two-factor three-level CCD design information, including details of factors, experimental data of three responses, quadratic regression models, verification, solution, further description of ^{1}H NMR spectrum of $mPEG_{113}$−PCC_{32}−VE_4, FT-IR spectrum, DSC, CMC, XRD, stability study, and pH-responsive profile. This material is available free of charge via the Internet at http://pubs.acs.org.

AUTHOR INFORMATION

Corresponding Authors

*Z.H.: tel/fax, +86-24-23986321; e-mail, hezhonggui@vip.163.com.
*Y.Z.: tel/fax, +86-24-23984219; e-mail, zhaiyinglei@aliyun.com.

Notes

The authors declare no competing financial interest.

ACKNOWLEDGMENTS

We gratefully acknowledge the kind help of Dr. Lianlong He (Shenyang National Laboratory for Materials Science, Institute of Metal Research, Chinese Academy of Sciences) in transmission electron microscopy visualization of our micelle samples. This work was financially supported by the National Nature Science Foundation of China (Grant Nos. 81173008, 81273450, and 81373336), the National Basic Research Program

DOI: 10.1021/bm501847u
Biomacromolecules XXXX, XXX, XXX−XXX

of China (973 Program, Grant No. 2015CB932100), and Program for New Century Excellent Talents in University (Grant No. NCET-753 12-1015).

REFERENCES

(1) Merisko-Liversidge, E.; Liversidge, G. G. *Adv. Drug. Delivery Rev.* **2011**, *63*, 427−440.
(2) Fahr, A.; Liu, X. *Expert Opin. Drug. Delivery* **2007**, *4*, 403−416.
(3) Lu, Y.; Park, K. *Int. J. Pharm.* **2013**, *453*, 198−214.
(4) Plapied, L.; Duhem, N.; des Rieux, A.; Préat, V. *Curr. Opin. Colloid Interface Sci.* **2011**, *16*, 228−237.
(5) Gaucher, G.; Satturwar, P.; Jones, M. C.; Furtos, A.; Leroux, J. C. *Eur. J. Pharm. Biopharm.* **2010**, *76*, 147−158.
(6) Schenk, M.; Mueller, C. *Best Pract. Res., Clin. Gastroenterol.* **2008**, *22*, 391−409.
(7) Deli, M. A. *Biochim. Biophys. Acta, Biomembr.* **2009**, *1788*, 892−910.
(8) Ganta, S.; Devalapally, H.; Shahiwala, A.; Amiji, M. *J. Controlled Release* **2008**, *126*, 187−204.
(9) Dai, J.; Nagai, T.; Wang, X.; Zhang, T.; Meng, M.; Zhang, Q. *Int. J. Pharm.* **2004**, *280*, 229−240.
(10) Jiang, H. L.; Zhu, K. J. *J. Appl. Polym. Sci.* **2006**, *99*, 2320−2329.
(11) Kunioka, M. *Macromol. Biosci.* **2004**, *4*, 324−329.
(12) Surnar, B.; Jayakannan, M. *Biomacromolecules* **2013**, *14*, 4377−43.
(13) Kim, S.; Kim, J. Y.; Huh, K. M.; Acharya, G.; Park, K. *J. Controlled Release* **2008**, *132*, 222−229.
(14) Filippov, S. K.; Starovoytova, L.; Konak, C.; Hruby, M.; Mackova, H.; Karlsson, G.; Stepanek, P. *Langmuir* **2010**, *26*, 14450−14457.
(15) Filippov, S.; Hruby, M.; Konak, C.; Mackova, H.; Spirkova, M.; Stepanek, P. *Langmuir* **2008**, *24*, 9295−9301.
(16) Leinonen, S.; Suokas, E.; Veiranto, M.; Tormala, P.; Waris, T.; Ashammakhi, N. *J. Craniofacial Surg.* **2002**, *13*, 212−218. For discussion, see: Mathy, J. A.; Warren, S. M.; Longaker, M. T. *J. Craniofacial Surg.* **2002**, *13*, 219−221. Eppley, B. L. *J. Craniofacial Surg.* **2002**, *13*, 222−223.
(17) Gunatillake, P.; Mayadunne, R.; Adhikari, R. *Biotechnol. Annu. Rev.* **2006**, *12*, 301−347.
(18) Nair, L. S.; Laurencin, C. T. *Prog. Polym. Sci.* **2007**, *32*, 762−798.
(19) Cady, R. B.; Siegel, J. A.; Mathien, G.; Spadaro, J. A.; Chase, S. E. *J. Biomed. Mater. Res.* **1999**, *48*, 211−215.
(20) Sinha, V. R.; Bansal, K.; Kaushik, R.; Kumria, R.; Trehan, A. *Int. J. Pharm.* **2004**, *278*, 1−23.
(21) Zhang, Z.; Kuijer, R.; Bulstra, S. K.; Grijpma, D. W.; Feijen, J. *Biomaterials* **2006**, *27*, 1741−1748.
(22) Seyednejad, H.; Ghassemi, A. H.; van Nostrum, C. F.; Vermonden, T.; Hennink, W. E. *J. Controlled Release* **2011**, *152*, 168−176.
(23) Schuller-Ravoo, S.; Feijen, J.; Grijpma, D. W. *Acta Biomater.* **2012**, *8*, 3576−3585.
(24) Dargaville, B. L.; Vaquette, C.; Peng, H.; Rasoul, F.; Chau, Y. Q.; Cooper-White, J. J.; Campbell, J. H.; Whittaker, A. K. *Biomacromolecules* **2011**, *12*, 3856−3869.
(25) Wu, R. Z.; Zhang, J. F.; Fan, Y. W.; Stoute, D.; Lallier, T.; Xu, X. M. *Biomed. Mater.* **2011**, *6*, No. 035004.
(26) Joseph, N. J.; Lakshmi, S.; Jayakrishnan, A. *J. Controlled Release* **2002**, *79*, 71−79.
(27) Lee, A. L. Z.; Ng, V. W. L.; Gao, S. J.; Hedrick, J. L.; Yang, Y. Y. *Adv. Funct. Mater.* **2014**, *24*, 1538−1550.
(28) Ke, X. Y.; Ng, V. W. L.; Gao, S. J.; Tong, Y. W.; Hedrick, J. L.; Yang, Y. Y. *Biomaterials* **2014**, *35*, 1096−1108.
(29) Tempelaar, S.; Mespouille, L.; Coulembier, O.; Dubois, P.; Dove, A. P. *Chem. Soc. Rev.* **2013**, *42*, 1312−1336.
(30) Constantinides, P. P.; Han, J.; Davis, S. S. *Pharm. Res.* **2006**, *23*, 243−255.
(31) Constantinides, P. P.; Tustian, A.; Kessler, D. R. *Adv. Drug. Delivery Rev.* **2004**, *56*, 1243−55.
(32) Cornaire, G.; Woodley, J.; Hermann, P.; Cloarec, A.; Arellano, U.; Houin, G. *Int. J. Pharm.* **2004**, *278*, 119−131.
(33) Elferink, R. P. J. O.; de Waart, R. *J. Physiol. Biochem.* **2007**, *63*, 75−81.
(34) Ai, X.; Sun, J.; Zhong, L.; Wu, C.; Niu, H.; Xu, T.; Lian, H.; Han, X.; Ren, G.; Ding, W.; Wang, J.; Pu, X.; He, Z. *Macromol. Biosci.* **2014**, *14*, 1415−1428.
(35) Wang, J.; Sun, J.; Chen, Q.; Gao, Y.; Li, L.; Li, H.; Leng, D.; Wang, Y.; Sun, Y.; Jing, Y.; Wang, S.; He, Z. *Biomaterials* **2012**, *33*, 6877−6888.
(36) Li, F.; Danquah, M.; Mahato, R. I. *Biomacromolecules* **2010**, *11*, 2610−2620.
(37) Danquah, M.; Fujiwara, T.; Mahato, R. I. *Biomaterials* **2010**, *31*, 2358−2370.
(38) Guan, H. L.; Xie, Z. G.; Tang, Z. H.; Xu, X. Y.; Chen, X. S.; Jing, X. B. *Polymer* **2005**, *46*, 5848−5848.
(39) Wang, Y. J.; Sun, J.; Zhang, T. H.; Liu, H. Z.; He, F. C.; He, Z. G. *Drug Dev. Ind. Pharm.* **2011**, *37*, 1225−1230.
(40) Feng, J.; Zhuo, R.-X.; Zhang, X.-Z. *Prog. Polym. Sci.* **2012**, *37*, 211−236.
(41) Chan, L. M.; Lowes, S.; Hirst, B. H. *Eur. J. Pharm. Sci.* **2004**, *21*, 25−51.
(42) Mei, L.; Zhang, Z.; Zhao, L.; Huang, L.; Yang, X. L.; Tang, J.; Feng, S. S. *Adv. Drug. Delivery Rev.* **2013**, *65*, 880−890.
(43) Montgomery, D. C. Response Surface Methods and Designs. *Montgomery Design and Analysis of Experiments*, 8th ed.; WILEY: New York, 2013; pp 478−554.
(44) Longo, G. S.; de la Cruz, M. O.; Szleifer, I. *ACS Nano.* **2013**, *7*, 2693−2704.
(45) Luo, C.; Sun, J.; Du, Y.; He, Z. *J. Controlled Release* **2014**, *176*, 94−103.
(46) Masaoka, Y.; Tanaka, Y.; Kataoka, M.; Sakuma, S.; Yamashita, S. *Eur. J. Pharm. Sci.* **2006**, *29*, 240−250.
(47) Merisko-Liversidge, E. M.; Liversidge, G. G. *Toxicol. Pathol.* **2008**, *36*, 43−48.
(48) Xu, W.; Ling, P.; Zhang, T. *J. Drug. Delivery* **2013**, *2013*, No. 340315.
(49) Alonso, M. J. *Biomed. Pharmacother.* **2004**, *58*, 168−172.
(50) Odeberg, J. M.; Kaufmann, P.; Kroon, K. G.; Hoglund, P. *Eur. J. Pharm. Sci.* **2003**, *20*, 375−382.
(51) Dintaman, J. M.; Silverman, J. A. *Pharm. Res.* **1999**, *16*, 1550−1556.
(52) Cornaire, G.; Woodley, J.; Hermann, P.; Cloarec, A.; Arellano, C.; Houin, G. *Int. J. Pharm.* **2004**, *278*, 119−131.
(53) Penninga, L.; M?ller, C. H.; Gustafsson, F.; Steinbruchel, D. A.; Gluud, C. *Eur. J. Clin. Pharmacol.* **2010**, *66*, 1177−1187.
(54) Wong, K. M.; Cheung, C. Y.; Chan, Y. H.; Chak, W. L.; Choi, K. S.; Chau, K. F.; Li, C. S. *Transplant. Proc.* **2000**, *32*, 1721−1722.
(55) Nassar, T.; Rom, A.; Nyska, A.; Benita, S. *J. Controlled Release* **2009**, *133*, 77−84.
(56) Collnot, E. M.; Baldes, C.; Schaefer, U. F.; Edgar, K. J.; Wempe, M. F.; Lehr, C. M. *Mol. Pharmaceutics* **2010**, *7*, 642−651.
(57) Turnberg, L. A.; Ross, I. N. *Scand. J. Gastroenterol. Suppl.* **1984**, *92*, 48−50.
(58) Phillipson, M.; Atuma, C.; Henriksnas, J.; Holm, L. *Am. J. Physiol.: Gastrointest. Liver Physiol.* **2002**, *282*, G211−G219.
(59) Livingston, E. H.; Engel, E. *J. Clin. Gastroenterol.* **1995**, *21* (Suppl 1), S120−S124.
(60) Ma, T.; Wang, L.; Yang, T.; Ma, G.; Wang, S. *Asian J. Pharm. Sci.* **2014**, *9*, 129−136.
(61) Junyaprasert, V. B.; Morakul, B. *Asian J. Pharm. Sci.* **2015**, *10*, 13−23.
(62) Wang, X. Q.; Zhang, Q. *Eur. J. Pharm. Biopharm.* **2012**, *82*, 219−229.

DOI: 10.1021/bm501847u
Biomacromolecules XXXX, XXX, XXX−XXX